Journal of Chromatography, 282 (1983) 263–286
Elsevier Science Publishers B.V., Amsterdam — Printed in The Netherlands

CHROMSYMP. 190

HIGH-PERFORMANCE LIQUID CHROMATOGRAPHIC COLUMN EFFICIENCY AS A FUNCTION OF PARTICLE COMPOSITION AND GEOMETRY AND CAPACITY FACTOR

R. W. STOUT* and J. J. DeSTEFANO
E. I. du Pont de Nemours & Co., Inc., Biomedical Products Department, Experimental Station, Wilmington, DE 19898 (U.S.A.)
and
L. R. SNYDER
Lloyd R. Snyder, Inc., 2281 William Court, Yorktown Heights, NY 10598 (U.S.A.)

SUMMARY

Reduced plate height (h) *vs.* reduced velocity (v) plots have been measured over a wide range of v for 36 high-performance liquid chromatographic systems. Column type was varied over wide limits and solute capacity factor (k') values were changed over the range 0.6–22. Resulting data can be accurately described by the Knox equation $h = Av^{1/3} + B/v + Cv$, where A is roughly constant (A = 0.5–0.8) for all columns studied, but values of B and C are strongly dependent on column type and solute k' values. These observations can be rationalized by a quantitative model that recognizes two effects: (a) surface diffusion of solute molecules in the stationary phase (along the pore wall) and (b) restricted diffusion of small solute molecules within particles having narrow pores and long alkyl chains bonded to their surface.

INTRODUCTION

The theory of band-broadening in high-performance liquid chromatography (HPLC) plays an important role in the understanding and use of the technique[1]. The early work of Giddings and of Knox[2–6] has both extended our understanding of band-broadening theory and simplified its application to method development and related optimization strategies[3,7–9]. In this connection, the so-called Knox equation is now widely used:

$$h = Av^{1/3} + B/v + Cv \tag{1}$$

where h is the reduced plateheight (H/d_p)*, v is the reduced mobile-phase velocity $(u\ d_p/D_m)$ and A, B and C are constants which describe a particular column. The term $Av^{1/3}$ reflects contributions to plateheight from mobile phase mass transfer plus

* See symbols at the end of this paper for definitions of commonly used symbols.

0021-9673/83/$03.00

flow anisotropy in the mobile phase; B/v is the result of longitudinal diffusion of solute, and Cv is the contribution from mass transfer within the packing particles (stagnant-mobile-phase mass transfer). One of the attractive features of eqn. 1 is that "good" columns are believed to have similar values of the constants A–C, which simplifies the practical application of this relationship; typical values for porous column packings are $A = 1$, $B = 2$, and $C = 0.02$–0.05 (refs. 4–6). Constancy in the values of A–C also allows the evaluation of a new column, the "goodness" of which can be assessed by how closely its values of A–C approach the latter values — or by whether they are still smaller.

Theory predicts that C in eqn. 1 should be a function of the solute capacity factor k' (ref. 2). Likewise, the parameter B should increase with k' if diffusion within the stationary phase is significant for a particular HPLC system[2,5]. The quantity A is normally assumed to be independent of k', although it may be a weak function of k' in some cases[6]. Only limited experimental data have been reported for the k'-dependence of A–C[4,5], so that *ab initio* predictions of A–C and of column performance as a function of k' have not been possible up to the present time. It is usually assumed that the dependence of A–C on k' can be ignored in practice, but optimization schemes which are based on this assumption must be considered approximate at best —and possibly in error in some cases.

It is likewise usually assumed that A–C are only weakly dependent on the composition of the stationary phase (silica, bonded phases, etc.) for the case of "good" columns. Thus, mass transfer into and out of the stationary phase is believed to be fast for silica, alumina and mono-layer bonded phases.

We have recently had occasion to question these prior assumptions concerning eqn. 1 as a result of our study of certain new column-packing materials and new column configurations[10]. Whereas the above discussion led us to expect similar plots of h *vs.* v for various columns described in ref. 10, we have in fact observed quite the opposite when experimental conditions were varied over wide limits: use of particles with different surface composition and pore diameter, variation of solute and/or mobile phase to change k', etc. This is illustrated in Fig. 1 for three such experimental systems: A, a narrow-pore silica column with k' equal about 12; B, a wide-pore C_8 column with k' also large (equal 17); C, the same column as in B, with k' equal to 0.6. Here it is seen that the individual h–v plots are by no means even roughly superimposable, reflecting large differences (in this case) in individual values of B and C. However, since all three plots exhibit minimum values of h in the range 1.6–2.2 particle diameters, all three columns would be classified as "good" columns by most workers.

A better understanding of eqn. 1 requires both an adequate experimental data base and attention to certain questions that have complicated previous attempts to measure and to interpret values of A–C for various HPLC systems. Specific points which require consideration in this regard include:

(1) Collection of sufficient data for each h–v plot (as in Fig. 1) with adequate precision and with correction for extra-column effect[10] so as to yield accurate values of A–C; measurement of h over a wide range in v and use of second-moment values of h.

(2) Study of a sufficient number of HPLC systems so as to allow the definition of the roles of k', particle composition and particle pore size in affecting values of A–C.

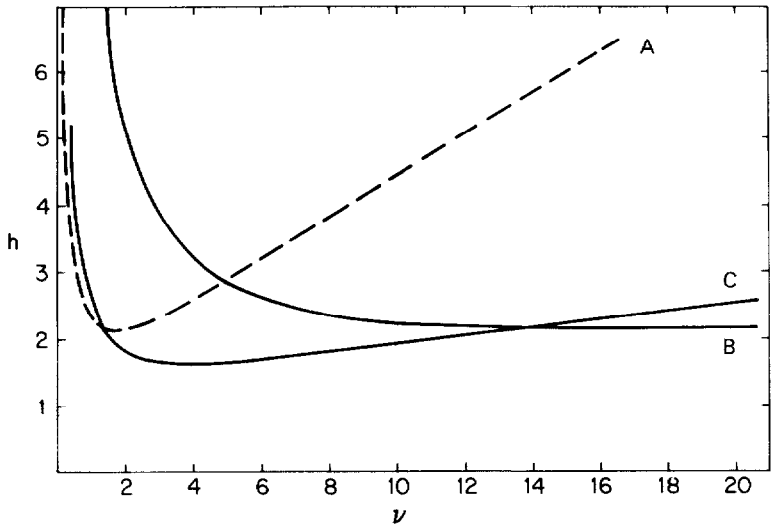

Fig. 1. Differences in h *vs* ν plots for different columns and/or different k' values of the solute. A, Zorbax-SIL, $k' = 11.6$; B, Zorbax-C_8 (17-nm-pore), $k' = 17$; C, same as B, $k' = 0.65$.

(3) Use of "good" particles of precisely defined geometry so as to minimize ambiguity in the interpretation of obtained value of A–C as a function of experimental conditions; restriction of columns tested to those that are well-packed, as evidenced by A-values in the range of 0.5–0.8 (ref. 10), so as to improve the precision of values of B and C.

(4) Reconciliation of all data collected in terms of a reasonable model of kinetic processes within the column, based on existing theory; so far as possible, our goal is a quantitative model that allows prediction of column efficiency (plate number N) as a function of all separation conditions.

The present paper describes a study carried out within the above guidelines. Concerning the use of "optimum" particles, we have chosen the column packing Zorbax (Du Pont). This packing material has a simple, well-defined geometry (microspheres bonded into a larger spherical particle[11]). Zorbax is also easily obtainable in very narrow particle size and pore-size distributions, and yields columns that are as efficient as any yet reported[10].

EXPERIMENTAL

Equipment, materials and procedures

These are described in detail in ref. 10. Chromatograms were made on a Du Pont Model 8800X HPLC system; the analog signal was fed to a PDP-10 system that provided for the determination of values of h, based on either a second-moments procedure or from the peak height/peak area ratio (first-moment value of h). Second-moment values of h were then corrected for both the extra-column volume of the system ($\sigma = 0.016$ ml) and for the system time-constant ($\tau = 0.20$ sec), as described in ref. 10 (eqns. 5a and b). Corrected values of h were finally fit by least-squares to eqn. 1, so as to obtain values of A–C; see Table I. Values of h for a

combination of (a) 3-μm particles, (b) high flow-rates and (c) small k' values were in some cases rejected because of excessive peak tailing and anomalously high values of h (second-moment). This effect is discussed further in Appendix I.

Derived values of A–C reported here are always for second-moment h values, unless noted otherwise. However, correlations of first-moment *vs.* second-moment data with eqn. 1 were carried out, and it was observed that close agreement of resulting A–C values generally resulted. Thus, for representative data from this study, second-moment values divided by first-moment values of A–C yielded the following ratios: A 1.12 ± 0.19; B, 1.00 ± 0.08; C, 1.07 ± 0.18. Likewise, correlation of second-moment h values with the reduced Van Deemter equation (eqn. 5 of ref. 12) was carried out for most sets of h–v data. As predicted by theory, resulting values of B and C agreed closely with those found for the corresponding application of the Knox equation (eqn. 1). Both the Van Deemter and Knox equations gave similar correlations with experimental h–v plots, with no significant overall difference in the error-of-fit in either case. To summarize, experimental values of B and C (and their interpretation) are essentially identical, whether first- or second-moment h values are used, or whether these data are fit to the Knox or reduced-Van Deemter equations.

Particle size and pore diameter measurements

The measurement of particle diameters was described in ref. 10, and is based variously on scanning electron microscopy (SEM) or transmission electron microscopy (TEM), augmented in some cases by column permeability measurements. Pore diameter values were obtained by nitrogen desorption for samples with pores smaller than 10 nm, and by arbitrarily averaging nitrogen desorption and mercury intrusion for packings with larger pores.

Columns

Zorbax-base columns were either commercial columns (Du Pont) or were prepared by us from research lots of Zorbax-SIL that were bonded with octyldimethylsilyl (C_8) or octadecyldimethylsilyl (C_{18}) and then slurry-packed into column blanks of various dimensions. The Perkin-Elmer 3-μm C_{18} column was purchased (Perkin-Elmer, Norwalk, CT, U.S.A), and the 5-μm C_8 and C_{18} columns from Supelco were the kind gift of Dr. R. Eksteen of Supelco (Bellefont, PA, U.S.A.).

Estimated diffusion coefficient (D_m) values

Analysis of the present experimental data in terms of eqn. 1 requires estimates of the solute diffusion coefficient D_m for each solute and mobile phase used. Our approach is based on the Wilke-Chang equation[1], using a composition-weighted value of solvent molecular weight and association factor where necessary[8]. Values of D_m for pentyl phthalate and 65–95% acetonitrile–water ranged from $6.9 \cdot 10^{-6}$ to $10.5 \cdot 10^{-6}$ cm^2/sec. Values of D_m for other phthalates were proportional to (solute mol. wt.)$^{-0.6}$, for the same mobile phase. For separations on silica, D_m values with methylene chloride as mobile phase were: benzanilide, $2.45 \cdot 10^{-5}$; *p*-bromoacetanilide, $2.4 \cdot 10^{-5}$.

RESULTS AND DISCUSSION

The data base collected during the present study is summarized in Table I. Values of h were measured for 11 different columns and a total of 36 different HPLC systems; this, in turn, generated 36 plots of h *vs.* v (followed by reduction of these plots to values of A, B and C). As can be seen, the experimental conditions of Table I encompass a wide range in particle type (silica, C_8, C_{18}, different pore diameters, different particle sizes), and provide variation in k' over the range $0.6 \leqslant k' \leqslant 22$. These data allowed us to examine the various questions posed in the Introduction.

Ideally, each system studied would provide for variation of v over a 20-fold range or greater for maximum accuracy in determining values of A–C. Such a plot is illustrated in Fig. 2a for the Zorbax-C_8 narrow-pore columns of Table I ($k' = 11.6$ and $d_p = 3.04$ and 5.67 μm). According to eqn. 1, data for both columns should fall on a single curve and this is seen to be the case. The dark circles and squares of Fig. 2a correspond to data points that were not included in the least-squares correlation with eqn. 1, as discussed in the Experimental section. However, the remaining points of Fig. 2a cover a range in v from 0.4 to 50, which is seen to be adequate for defining the overall curve and resulting values of A–C.

In other cases, the range of v covered was less than in Fig. 2a for reasons of convenience or because of the rejection of data points at higher values of v. Such an example is shown in Fig. 2b, for Zorbax-SIL ($k' = 11.6$) and d_p equal both 3.04 and 5.67 μm.

Goodness of fit of h–v data to Knox equation

The relative ability of eqn. 1 to correlate experimental values of h *vs.* v is illustrated in Fig. 2 and Table I. The least-squares error-of-fit to eqn. 1 averaged 0.17 units in h, over a range in h values of about $2 \leqslant h \leqslant 10$. Eqn. 1 also requires that values of A–C remain constant for a given HPLC system as particle size, d_p, is varied, and this was generally observed, except for the case of A-values for small k', small d_p values (see Appendix I)*.

Values of A–C for a given system but varying d_p are compared in Table II, to check the ability of eqn. 1 to predict accurately the effect of d_p on column plate number. The basic theory behind eqn. 1[2–6] predicts the A–C will be independent of d_p, and this is noted to be approximately true in Table II. Exceptions noted in Table II can for the most part be attributed to small differences in pore diameter between packing-lots of varying d_p (these lots were prepared individually, rather than being screened from single lots of polydisperse particles). Limitations of the data sets used for evaluating A–C (*cf.* C-term of Fig. 2b) could also lead to imprecision in the determined values of A–C.

Values of B in the Knox equation —stationary phase or surface diffusion

The assumption that axial diffusion occurs with the same mobile phase dif-

* Resulting values of A–C for the case of estimated A values are shown in parentheses in Table I; these are the values used in the following discussion, as we feel they are more accurate. In experiments where values of A were believed to be inaccurate, estimated values of A could be obtained from related experiments on the same column (Appendix I).

TABLE I

SUMMARY OF COLUMN PLATEHEIGHT DATA OBTAINED IN PRESENT STUDY

Second-moment values of h, least-squares fit to eqn. 1. Values of D_m from Wilke-Chang equation[1,8].

*Column**	d_p (μm) (pore diam. in nm)	*Solute***	*Mobile phase****	k'	*Knox parameters*§				*Range in v*	n§§	ρ
					A	*B*	*C*	*Error of fit*			
Zorbax silica	3.04 (6)	BA	MC	2.3	0.32 (0.76)§§§	1.02 (0.91)	0.53 (0.38)	±0.04 (0.09)	0.5 5	17	0.71
		pBA	MC	11.0	0.79	1.27	0.32	0.02	0.4 6	17	0.44
	5.67	BA	MC	2.6	0.68	1.00	0.29	0.13	0.6 8	19	0.91
	(7.5)	pBA	MC	12.2	0.73	1.27	0.22	0.02	0.6 17	19	0.60
Zorbax C_8	3.04 (6)	C_5	85 ACN	2.4	0.25 (0.55)	3.0 (2.9)	0.13 (0.06)	0.16 (0.27)	0.3 14	46	0.56
		C_8	85 ACN	11.3	0.50	5.2	0.03	0.25	0.4–17	64	0.38
	5.67 (7.5)	C_5	85 ACN	2.6	0.44 (0.55)§§§	3.6 (3.6)	0.07 (0.06)	0.10 (0.15)	0.4–51	64	0.54
		C_8	85 ACN	11.9	0.59	5.0	0.03	0.16	0.5–64	79	0.37
	4.0 (17)	C_4	85 ACN	0.65	(0.66)§§§	1.9	0.04	0.09	1.3 10	10	1.05
		C_5	85 ACN	0.97	(0.66)§§§	2.1	0.04	0.26	1.4 16	12	1.01
		C_4	70 ACN	2.0	(0.66)§§§	3.4	0.035	0.17	1.7–20	14	0.94
		C_5	70 ACN	3.4	(0.66)§§§	4.5	0.032	0.13	1.7 33	16	0.78
		C_8	85 ACN	3.4	0.66	3.6	0.045	0.09	2 42	16	0.56
		C_8	70 ACN	17.0	0.66	8.7	0.00	0.20	2–43	16	–

Zorbax C_{18}	3.04	C_5	95 ACN	1.4	(0.55)[§§§]	1.4	0.30	0.02	3–9	3	0.16
	(6)		91 ACN	2.1	(0.55)[§§§]	2.3	0.18	0.08	0.4–9	37	0.23
			90 ACN	2.3	(0.55)[§§§]	2.9	0.23	0.18	3–18	5	0.17
			85 ACN	3.6	(0.55)[§§§]	4.4	0.15	0.20	4–20	5	0.20
			80 ACN	5.5	(0.55)[§§§]	2.8	0.12	0.11	4–22	5	0.19
			75 ACN	8.4	(0.55)[§§§]	4.0	0.08	0.23	4–24	5	0.21
			70 ACN	12.9	(0.55)[§§§]	7.8	0.04	0.17	5–26	5	0.29
			65 ACN	19.9	(0.55)[§§§]	9.0	0.03	0.38	5–28	5	0.26
		C_8	91 ACN	12.8	0.54	3.5	0.07	0.44	1–55	60	0.17
	5.8	C_4	91 ACN	1.4	(0.50)[§§§]	2.6	0.10	0.18	1.5–14	12	0.48
	(9)	C_5	91 ACN	2.4	(0.50)[§§§]	2.4	0.08	0.17	1.6–32	17	0.48
		C_8	91 ACN	13.4	0.50	5.2	0.03	0.12	2–35	14	0.37
	5.8[†]	C_5	91 ACN	2.4	0.49	2.6	0.085	0.06	1.7–51	19	0.45
	(9)	C_5	88 ACN	3.3	0.49	4.0	0.095	0.28	1.7–54	18	0.34
		C_8	91 ACN	14.0	0.69	4.0	0.035	0.16	2–85	25	0.31
		C_8	88 ACN	21.5	0.54	6.6	0.04	0.26	2–66	18	0.18
Perkin-Elmer C_{18}	3.2[††]	C_5	88 ACN	1.8	0.40	2.5	0.19	0.08	0.4–10	34	0.29
	(9)				(0.73)	2.3	0.13	0.26			
		C_8	88 ACN	10.7	0.73	4.3	0.05	0.11	0.5–33	52	0.24
Supelco C_8	5.2[†]	C_5	87 ACN	2.4	0.75	4.0	0.07	0.11	1.6–60	19	0.48
	(11)	C_8	87 ACN	12.3	0.72	5.9	0.03	0.12	1.5–104	20	0.36
Supelco C_{18}	5.2[†]	C_5	87 ACN	1.9	0.75	5.0	0.10	0.14	1.6–41	31	0.38
	(11)	C_8	87 ACN	11.7	0.86	5.8	0.03	0.21	2–69	38	0.37

[*] Source and surface composition indicated; column dimensions 8 × 0.62 cm, unless indicated otherwise in second column (see footnotes [†] and [††].
[**] BA = Benzanilide; pBA = *p*-bromoacetanilide; C_4, C_5 and C_8 refer to di-*n*-alkylphthalate (*e.g.*, C_4 is di-*n*-butylphthalate).
[***] MC = Methylene chloride; 85 ACN = acetonitrile water (85:15) etc.
[§] Least-squares fit to eqn. 1; *A* values in parentheses are predetermined (see Appendix I).
[§§] Number of data points (h–v pairs) fit to eqn. 1.
[§§§] Predetermined value of *A* (see Appendix I).
[†] 15 × 0.46 cm Column.
[††] 10 × 0.46 cm Column.

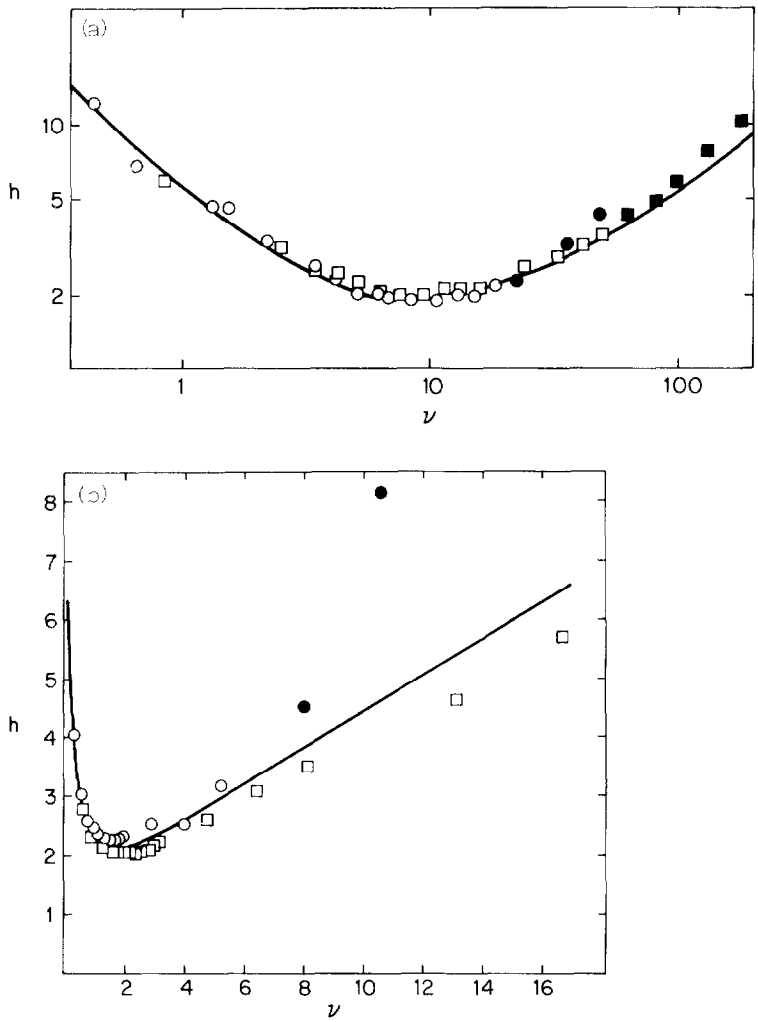

Fig. 2. Examples of the fit of experimental data to the Knox equation (eqn. 1). (a) Data for Zorbax-C_8 columns (6-nm-pore) with d_p = 3.04 μm (○) and 5.67 μm (□); k' = 11.6; (b) Zorbax-SIL columns with d_p = 3.04 μm (○) and 5.67 μm (□), k' = 11.6. Dark points are rejected, as discussed in the Experimental section. For other details, see Table I.

fusion coefficient D_m inside and outside the particle can be combined with the Einstein equation[2] to give

$$B = 2\gamma \tag{2}$$

where γ is a tortuosity factor that is an average of values for the regions inside and outside of the particle. Knox cites average values of γ equal to 0.8–1.0 for porous particles[4], although values of B as low as 1.2 (implying γ = 0.6) have been reported for pellicular packings[13]. Most workers assume that γ = 1, and B can then be taken as 2[4,6,14,15].

TABLE II

CONSTANCY OF VALUES OF A, B OR C AS ONLY d_p IS VARIED

Data from Table I for Zorbax columns.

Column type	k'	d_p*	A	B	C
Silica	2.4	3.04	−**	0.91	0.38***
		5.67	0.68	1.00	0.29
	11.6	3.04	0.79	1.27	0.32***
		5.67	0.73	1.27	0.22
C_8	2.5	3.04	−**	2.9	0.06
		5.67	−**	3.6	0.06
	11.6	3.04	0.50	5.2	0.03
		5.67	0.59	5.0	0.03

* Average of k' values in Table I.

** Less accurate value, with predetermination of A in the data-set correlation.

*** The higher value of C for the 3-μm *vs.* 5.7-μm silica particles is believed to arise from the smaller pores (6 nm) in the former *vs.* the latter (7.5 nm); see Table V and discussion in text.

It can be seen in Table I that values of B measured by us are generally not equal to 2, and are often much larger. It is further observed that larger values of B correlate with larger values of k', as would be predicted by additional diffusion within the stationary phase (involving surface diffusion along the walls of the pore)[2].

Previous workers have observed at various times that diffusion in the stationary phase can provide a possible contribution to B[5,7,16], in which case eqn. 2 is expanded[2] to give

$$B = 2\,[\gamma + \gamma_s\, k'\, (D_s/D_m)] \tag{3}$$

where γ_s is the tortuosity factor that applies to the pore wall or stationary phase, and D_s is the solute diffusion coefficient in the stationary phase. Some workers have apparently assumed $D_s = D_m$ and $\gamma = \gamma_s$ for certain systems, in which case[6]

$$B = 2\gamma\,(1 + k') \tag{3a}$$

However, eqn. 3a should not be generally applicable.

Experimental data showing larger values of B than are predicted by eqn. 2 have been reported by several workers[5,16,17], suggesting the importance of surface diffusion (eqn. 3) in at least some HPLC systems. However, in most cases, larger B values have been blamed on experimental imprecision[5] or attributed to other effects; *e.g.*, diffusion of solute to the column wall[17]. Thus, the possibility of surface diffusion as a contributor to the B term of eqn. 1 is frequently ignored*. The relative lack of interest in surface diffusion is probably due to the lack of importance of B in practical

* More recently, Chen *et al.*[18] state that, "We are unaware of data which demonstrate a strong dependence of the B term on k'...", while Knox *et al.*[19] find (as we do) that the opposite is true in systems similar to those reported on here.

separations involving particles of 5-μm diameter or larger. Here, large v values are typical, and values of h are relatively insensitive to values of B. However, there are two reasons why values of B are more important than had been considered earlier. First, the use of very-small-particle packings (*e.g.*, 3-μm, as in ref. 10) leads to smaller values of v in practice, and the effect on h of larger values of B (according to eqn. 3) is then more significant. Second, previous workers appear to have overlooked the fact that larger values of B (due to surface diffusion) should lead to smaller values of C as a result of faster mass transfer (or effective diffusion) within the particle pores.

Returning to the effect of surface diffusion on B, eqn. 3 can be expanded so as to differentiate solute diffusion in mobile phase that is either outside the particle (o) or inside the particle pores (p):

$$B = 2 [x \gamma_o + (1 - x)\gamma_p (D_p/D_m) + k' \gamma_s (D_s/D_m)] \quad (4)$$

Here, x is the fraction of mobile phase within the column that is outside the particles, γ_o and γ_p are tortuosity factors outside the particle and inside the pores, respectively, and D_p is a solute diffusion coefficient for diffusion in the mobile phase inside the pores.

The value of γ appropriate to porous particles, such as Zorbax, has been examined in detail by Knox and McLaren[20]. On the basis of this analysis and recent data[19], Knox favors a value of $\gamma = 0.9$ for most packings. However, the exact value of γ for these packings has little effect on the following discussion. According to ref. 19, γ should be smaller for lower-pore-volume packings, such as Zorbax, and we presently favor a value of $\gamma = 0.64$ for Zorbax-type packings. We will assume that $\gamma_o = \gamma_p = \gamma_s = 0.64$. Eqn. 4 can then be rewritten for Zorbax-type particles as

$$B = 1.28 [x + (1 - x)(d_p/D_m) + k' (D_s/D_m)] \quad (4a)$$

We might also expect that eqn. 4a can serve as a first approximation for other kinds of HPLC particles.

TABLE III

VALUES OF THE FRACTION x OF MOBILE PHASE OUTSIDE THE PARTICLES FOR VARIOUS COLUMNS OF TABLE I

Column	x		
	*calc.**	*calc.***	*best*
Zorbax-SIL	0.63	0.63	0.63
Zorbax C_8 (narrow-pore)	0.74	0.76	0.75
Zorbax C_8 (wide-pore)	0.67		0.67
Zorbax C_{18}	0.82	0.79	0.80

* Based on calculated volume of bonded phase inside particle.

** Based on experimental value of V_m.

For Zorbax-like particles with interparticle void-fraction 0.40 times the volume of the column blank, we can estimate values of x for a given column in various ways. For non-bonded silica, the above discussion suggests that if the volume fraction V_o outside the particles is 0.4, then the volume fraction inside the particle V_p will be 0.4 $\times$ 0.6 = 0.24, and x will equal 0.4/(0.4 + 0.24) = 0.63. Knowing the surface coverage of a particle, the value of V_p can be corrected for partial filling by bonded phase, and a value of x calculated for various bonded-phase columns. Alternatively, the total volume of mobile phase in the column (V_m) can be determined, whereupon

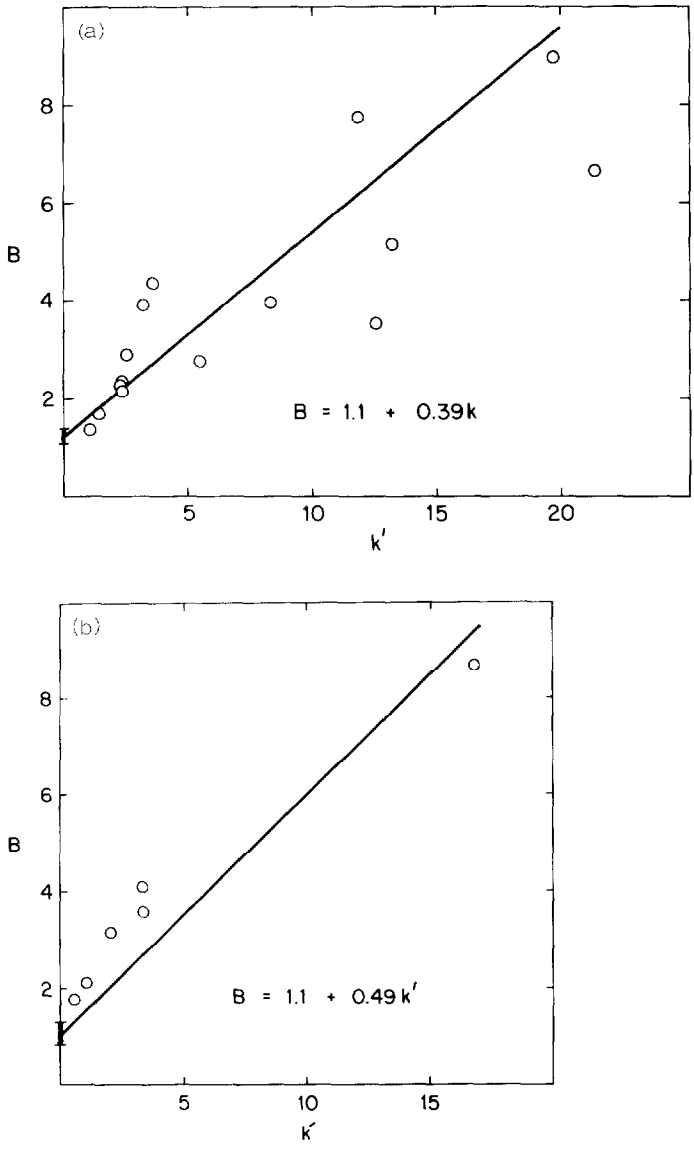

Fig. 3.

(*Continued on p. 274*)

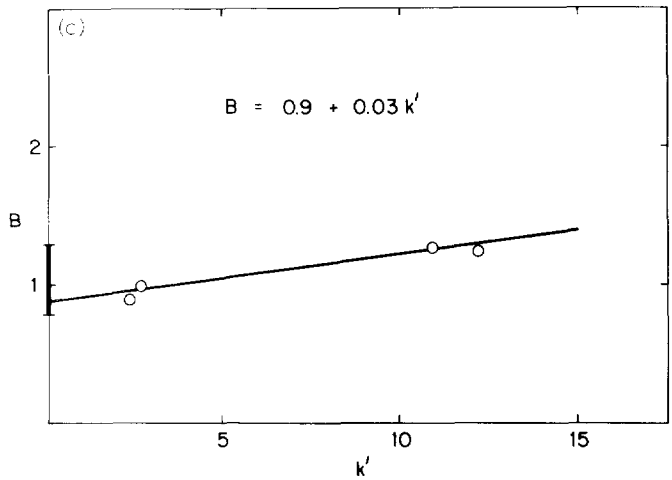

Fig. 3. Variation of the Knox parameter B with k'. Data from Table I. (a) Data for 6-nm Zorbax C_{18} column; (b) data for 17-nm Zorbax C_8 column; (c) data for 6-nm Zorbax-SIL column.

if V_m is expressed as a volume fraction, $x = 0.4/V_m$. Table III sumarizes these various calculations for some of the columns of Table I, with "best" (average) values of x shown in the column on the right of Table III.

The dependence of B on k' predicted by eqn. 4a is tested in Fig. 3 for several columns from Table I. It is expected that generally $D_p \leqslant D_m$, so that the intercept ($k' = 0$), predicted from eqn. 4a, will fall between $1.28x$ and 1.28. This interval is indicated for the various plots of Fig. 3 as the dark line on the B-axis for each plot. For the bonded-phase columns of Fig 3a (C_{18}-narrow-pore) and Fig. 3b (C_8-wide-pore), a clear increase in B with increase in k' is observed. The slopes of the two plot are similar (0.39–0.49) and may be the same within experimental error. The value of the slopes (*cf.* eqn. 4a) suggests that surface diffusion is important in these systems, and D_s/D_m lies between 0.4 and 0.5. Other bonded-phase columns in Table I show a similar increase in B with k', but the experimental uncertainty in B does not permit us to claim any significant variation in D_s/D_m for these columns.

Fig. 3c shows the dependence of B on k' for the two silica columns of Table I. Here, it is apparent that the significance of surface diffusion is much less, reflecting an apparent value of $D_s/D_m = 0.03$; *i.e.* one tenth of the value for the bonded-phase columns. In the absence of further experimental data, it is believed that the much slower surface diffusion of the phthalate solutes on silica is due to the localization of these molecules on surface silanol groups[21–23].

Finally, it should be noted that the scatter of data in Fig. 3 is such that it is impossible to determine the precise intercept on the B-axis and thereby determine D_p/D_m from eqn. 4a. Information concerning the value of D_p is more readily accessible from a theoretical analysis of the C values of Table I, as is discussed in the next section.

Values of C in the Knox equation —the significance of surface diffusion in promoting mass transfer

For the porous, small-particle columns, which are mainly used at present, most workers attribute the C term of eqn. 1 to stagnant-mobile-phase effects. An exact expression for C can be derived for this case[2]:

$$C = [1/30\gamma(1 - x)][(1 + k' - x)/(1 + k')]^2 \quad (5)$$

For representative values of $x = 0.64$ and $\gamma = 0.64$, eqn. 5 predicts the following values of C: $k' = 0.0$, $C = 0.02$; $k' = 1.0$, $C = 0.07$; $k' = 3.0$, $C = 0.10$; $k' = 10.0$, $C = 0.13$. Thus, C is expected generally to increase with k'.

Some reports suggest that "good" columns show rough agreement between experimental values of C and values from eqn. 5 (ref. 5). However, previous discussions of the theoretical basis of the C term have been confused by the use of several variations on eqn. 5; thus, Knox uses at least four different equations for C, at least some of which are not mathematically equivalent[4–6,13]. Other workers have used a different model for the C term, based on diffusion within a uniform sphere[2]:

$$C = (1/30)[k'/(1 + k')^2](D_m/D_s) \quad (5a)$$

In principle, either of these two models should be adaptable so as to describe an actual HPLC system, but eqn. 5 seems the better starting point.

Fig. 4 plots C values *vs.* k' for several columns in Table I. Each of these curves *decreases* with k' (for $k' \gtrsim 1$), whereas, eqn. 5 predicts an *increase* in C as k' increases. Furthermore, values of C for different columns and the same value of k' are seen to vary widely —by more than a factor of 20 in some cases, which is a much larger variation than is predicted from eqn. 5. We believe that the decrease in C with in-

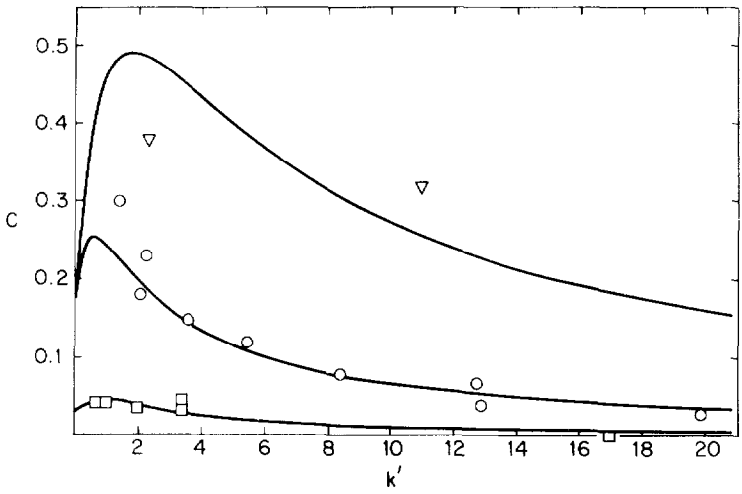

Fig. 4. Variation of the Knox parameter C with k'. Data from Table I. ▽, Data for 6-nm Zorbax-SIL column; ○, data for 6-nm Zorbax C_{18} column; □, data for 17-nm Zorbax C_8 column. Solid curves are calculated from eqn. 8a, as described in the text, by use of data from Tables IV and V.

creasing k' is due to surface diffusion, as postulated in the last section to explain the increase in B with k' for most of the systems of Table I. Thus, if the effective diffusion coefficient of sample molecules is greater within the particle pores as a result of surface diffusion, the value of C found should be proportionately less.

Only part of the difference in C values for different columns can be attributed to the effects of surface diffusion. An additional contribution is due to restriction of solute diffusion in narrow pores, or within intra-particle regions where diffusion is impeded by steric effects.

Expansion of eqn. 5 to include the effects of surface and/or restricted diffusion

The B term of eqn. 1 can be rewritten in unreduced form as

$$H = 2\gamma D_m/u \tag{6}$$

We can postulate an effective diffusion coefficient $\tilde{D}_p$ within the particle such that

$$H = 2\gamma[x\, D_m + (1 - x)\, \tilde{D}_p]/u \tag{6a}$$

where the term $x\, D_m$ is the contribution to total diffusion from molecules outside the particle and $(1 - x)\tilde{D}_p$ is the remaining contribution from molecules inside the particle. Reconverting eqn. 6a to the reduced form ($H = h\, d_p$, $v = u\, d_p/D_m$) and considering only longitudinal diffusion ($h = B/v$), we then have from eqn. 6a

$$B = 2\gamma[x + (1 - x)\, (\tilde{D}_p/D_m)] \tag{6b}$$

so that

$$\tilde{D}_p = [(B/2\gamma) - x]D_m/(1 - x) \tag{7}$$

From eqn. 4a we can express B as a function of k':

$$B = a + b\, k' \tag{7a}$$

where the constants a and b (for a given HPLC system) can be evaluated from experimental plots, as in Fig. 3.

The C term of eqn. 1, as expressed by eqn. 5, can be expanded to correct for the greater diffusion within the particle (due to surface diffusion) by multiplying C by the ratio $(D_m/\tilde{D}_p)$:

$$C = [1/30\gamma(1 - x)]\, [(1 + k' - x)/(1 + k')]^2(D_m/\tilde{D}_p) \tag{8}$$

Thus, if the effective diffusion coefficient inside the pore $(\tilde{D}_p)$ is greater than the diffusion coefficient in the external mobile phase (D_m), the mass transfer in and out of the particle will be correspondingly greater and C will be proportionately smaller.

Additionally, we must consider the possibility of restricted diffusion within the particle pores, when the size of solute molecules is similar to the cross section of the pores[24]. Several workers have reported plateheight values for macromolecular solutes

(mol.wt. > 2000 daltons), finding generally that the solute diffusion coefficient within the pore can be 6- to 50-fold smaller than the corresponding D_m value in the mobile phase outside the particle[25–28]. We believe such effects are of minor importance for small-molecule solutes. However, another kind of restricted diffusion inside particle pores is possible, in which changes in solute diffusion coefficient have a greater effect on C of the Knox equation than on B. It is essential in this regard that we distinguish intra-particle diffusion in two regions within the particle, as illustrated in Fig. 5a. The sample molecules (solid dots in Fig. 5a) are to be found in the pore channel (i), on the microparticle surface (pore wall, ii) and at the junctures of microparticles (iii). Presumably diffusion will be slower in region iii *vs.* regions i plus ii, and at any time most of the sample molecules will be found in regions i plus ii.

As a result of steric interaction and/or pore-size effects, we can postulate a restriction factor ρ that reduces the effective diffusion coefficient $\tilde{D}_p$ for regions i plus ii to a new value $\tilde{D}_p\rho$ in regions i plus ii plus iii. Now the B term of eqn. 1 will be determined mainly by the value of $\tilde{D}_p$ in regions i plus ii, where most of the sample molecules are to be found at any given time. The C term, on the other hand, is affected significantly by slow diffusion and mass transfer in region iii (see Appendix II). Eqn. 8 already recognizes restricted diffusion in regions i plus ii because $\tilde{D}_p$ is

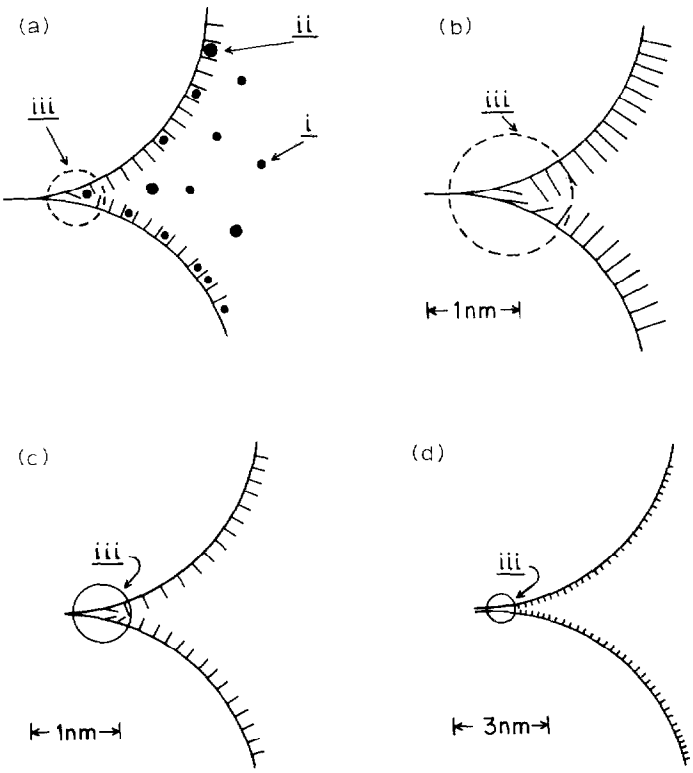

Fig. 5. Visualization of solute diffusion within the pore structure of a particle. Cross section of bonded-phase microparticles shown. ●, Solute molecules. (a) Illustration of diffusion in pore liquid (i), pore wall (ii) and restricted regions (iii); (b) C_{18} small-pore particle; (c) C_8 small-pore particle; (d) C_8 large-pore particle.

determined experimentally from the value of B (eqn. 7). So we must expand eqn. 8 to recognize restricted diffusion in region iii *vs.* regions i plus ii by multiplying $\tilde{D}_p$ by the restriction factor ρ ($\rho \leqslant 1$):

$$C = [1/30\gamma(1 - x)]\,[(1 + k' - x)/(1 + k')]^2\,(D_m/\tilde{D}_p\rho) \tag{8a}$$

In figs. 5b d we further explore the relative restriction of diffusion in region iii as a function of the particle geometry and surface composition. Fig. 5b portrays the nature of region iii for a small-pore particle with a C_{18} (*i.e.*, long) alkyl chain. Fig. 5c shows the same particle with a C_8 chain, and Fig. 5d shows a large-pore C_8 particle. It is apparent from these diagrams that the extent of restricted diffusion should decrease as pore size increases and/or as alkyl-chain length decreases; *i.e.* ρ should approach 1 for larger-pore, shorter-chain particles. It should also be apparent from Fig. 5 that restricted diffusion, as defined by the parameter ρ, may be more important for smaller solute molecules. Thus, larger solute molecules may be sterically excluded from region iii. A similar discussion has been given by Chen *et al.*[18] to explain certain data obtained by them in LC systems similar to those studied here.

Comparison of data of Table I with eqn. 8a

We can now calculate values of the restriction factor ρ for the various systems of Table I (summarized in last column of Table I). Our approach is to express B as a function of k' via eqn. 7a, calculate $(\tilde{D}_p/D_m)$ from values of B, γ and x from eqn. 7, and then calculate ρ from eqn. 8a by using values of γ and x summarized previously (Table III) plus experimental values of k' and C. The resulting values of ρ should be constant for a given column (as a first approximation) and should vary with particle type, as discussed for Fig. 5; *i.e.* ρ should be close to 1 for large-pore short-alkyl-chain packings, and ρ should decrease with increase in alkyl-chain length and/or decrease in pore diameter.

Values of ρ as determined in the above manner, are tabulated in the last column of Table I, and Table IV provides a summary of these data for individual columns. The data of Table IV can be used to test the reliability of eqn. 8a when ρ is assumed

TABLE IV

AVERAGE VALUES OF THE RESTRICTION FACTOR ρ FOR VARIOUS COLUMNS OF TABLE I

*Column**	*Pore diameter (nm)*	ρ		
		Silica	C_8	C_{18}
Zorbax (3.04)	6	0.58 ± 0.20	0.47 ± 0.13	0.21 ± 0.04
Zorbax (5.67)	7.5	0.75 ± 0.22	0.45 ± 0.12	
Zorbax (5.8)	9			0.35 ± 0.10
Zorbax (4.0)	17		0.87 ± 0.19	
Perkin-Elmer (3.2)	9**			0.27 ± 0.04
Supelco (5.2)	11**		0.42 ± 0.09	0.37 ± 0.01

* d_p in parentheses, see Table I.

** Estimate from Vendor.

to be constant for a particular column type. First, we see in Table IV that values of ρ for a given column are consistent with eqn. 8a, showing an average coefficient of variation of 23%. These values of ρ are proportional to experimental values of C (eqn. 8a), and the latter are unlikely to be more accurate than $\pm 20\%$. A second way of demonstrating the ability of eqn. 8a to correlate and predict values of C and ρ for different columns is by comparing experimental values of C with values calculated from eqn. 8a with a best-fit value of ρ. The solid curves of Fig. 4 are, in fact, calculated in this fashion.

Another test of whether the ρ values of Table IV are reasonable is to examine how experimental ρ values correlate with particle pore diameter and alkyl-chain length of the bonded phase. Fig. 5 suggests that ρ should decrease as pore diameter decreases and alkyl-chain length increases. Because many of the ρ values in Table IV are based on only two h–v plots from Table I, the corresponding averages of Table IV are less precise. We can further group (or average) several of the ρ values of Table IV to improve the accuracy of final ρ values (see Table V).

For the 6- to 7.5-nm-pore packings (Table V) ρ decreases in going from silica (0.62) to C_8 (0.46) to C_{18} (0.21); *i.e.*, smaller values of ρ result from greater filling of the pore network by bonded phase. Likewise, ρ increases for columns of the same type as the pore diameter increases: (a) from ρ equal 0.46 to 0.87 for C_8 Zorbax, as pore diameter increases from 6–7.5 nm to 17 nm; (b) from ρ equal 0.21 to 0.35 for C_{18} Zorbax, as pore diameter increases from 6 to 9 nm. For the 17-nm-pore C_8 Zorbax, the observed value of ρ (0.87) is close to unity, as expected for this less restricted pore network.

Data are also summarized in Table IV for columns obtained from other manufacturers (Supelco, C_8 and C_{18}; Perkin-Elmer, C_{18}). The ρ values for these three columns are in line with values for similar Zorbax columns.

Values of $\tilde{D}_p$, as determined from B *vs.* k' (Fig. 3), are also expected to be somewhat sensitive to restricted diffusion (see Fig. 5). There is some experimental verification of this assumption in that restricted diffusion of solute molecules in regions ii plus iii of Fig. 5 should lead to a decrease in the parameter b of eqn. 7a. This is observed for the 17-nm-pore Zorbax C_8 ($b = 0.49$) *vs.* the more restricted 6-nm-pore Zorbax C_{18} ($b = 0.39$). However, the difference in b is only 20%. The corresponding change in ρ for these two columns is four-fold, reflecting a much greater response of C-term-related diffusivity to pore-restriction effects *vs.* B-term-related diffusivity. On the basis of these observations for extremes in pore diameter and chain length, we assume that b will equal roughly 0.44 for the other bonded phase columns of Tables I and IV, and that b will in general not exceed a value of 0.5. An

TABLE V

AVERAGE ρ VALUES FROM TABLE IV

Packing pore diameter (nm)	*Average value of ρ for different chain lengths*		
	Silica (C_0)	C_8	C_{18}
6–7.5	0.62	0.46	0.21
9			0.35
17		0.87	

example of the derivation of values of ρ and calculation of values of C is given in Appendix III.

Practical implications of surface diffusion and restricted diffusion in HPLC packings

We can draw a number of conclusions from the preceding observations. First, the combination of pore diameters less than 10 nm with longer alkyl-chain bonded-phases (C_{18}) leads to a three- to five-fold decrease in $\tilde{D}_p$ and increase in C. This, in turn, adversely affects the efficiency of such columns, particularly at higher flow-rates and for solutes of higher molecular weight (and lower D_m). Suspicions that this is the case are common among experienced workers, but we are aware of only a few publications that present data on this effect. Halász and co-workers[29] observed no effect of pore diameter or alkyl-chain length on column efficiency, when pore diameters were 10 nm or larger. Engelhardt *et al.*[30], on the other hand, found an increase in plateheight for retained solutes when the pore diameter of silica was successively decreased from 13 nm to 6 nm to 4 nm (*cf.* ref. 30a).

Second, surface diffusion of solute molecules definitely occurs in the bonded-phase packings studied here. The apparent surface diffusion coefficient, D_s, is about half as large as the bulk liquid diffusion coefficient, D_m. Other workers[5–7] have stated that surface diffusion exists, and Horváth[31] reports that values of D_s and D_m are of comparable magnitude. However, there has been no experimental validation of this effect in previous studies of HPLC packings. The present study clarifies this question for systems of interest in HPLC (*cf.* ref. 19). Interestingly, the extent of surface diffusion was observed to be much smaller for the silica column studied by us than for corresponding bonded-phase columns. We believe this to be due to localization of polar solute molecules on the silica surface.

Third, the optimum reduced velocity for minimum h varies with k' for the solute. This can be seen in Fig. 1 for the C_8 column, B ($k' = 17$) *vs.* C ($k' = 0.7$), where for this range in k' the optimum value of v varies from 4 to >20. This effect has only a minor impact on the optimum solvent strength for a given separation, in that maximum effective plates per unit time will occur for larger values of k' than are normally assumed [*i.e.*, $2 \leqslant k' \leqslant 5$ (ref. 32)]. More significantly, the dependence of optimum v on k' will typically yield lower values of N for compounds of smaller k'. This has been observed by other workers (*e.g.*, Fig. 8 of refs. 33 and 34) and is often attributed to extra-column effects. However, the decrease in N at lower k' can also arise from the column per se (as in Fig. 1). Thus, it is risky to assume that extra-column effects are important just because N decreases for solutes with lower k' values.

Fourth, on the basis of the present treatment, it is possible to predict values of A–C for a given HPLC system (with a "good" column) with much greater accuracy than previously. This, in turn, allows us to design columns of optimal configuration for general application. Wider-pore particles and shorter-chain bonded phases can provide generally greater column efficiencies, particularly at higher flow-rates and faster separations.

Fifth, the present study provides a basis for a closer look at column efficiency for macromolecular solutes, such as proteins. It is often assumed that "real" samples of any kind will yield lower values of N than are obtained for model compounds of the type tested here (*i.e.*, phthalates). It is further assumed that large peptides and

proteins will give still lower values of N for various reasons. There are reasons to doubt these generalizations, and this is a subject of ongoing investigation in this laboratory.

Several observations can be made at this point. We have shown earlier[10] that columns similar to those used here give the same N values for all samples so far studied. Specifically, for the separation of PTH-amino acids on a phenethyl-bonded-phase column similar to the 3-μm 6-nm-pore columns of Table I, values of h were found equal to 2 for later-eluted solutes. Other studies[4,5] have generally shown that C increases with k' —the opposite of what we observe. We believe that larger C terms for "real" samples and larger k' values generally reflect secondary retention processes within the packing. In most cases, these effects can be suppressed by chemical modification of the mobile phase (*e.g.*, addition of triethylamine–acetic acid[35]), including the use of ion pairing[36]), which gave reduced h values close to 2 for polar amphoteric solutes, such as the amino sulfonic acids. Another study[37] of the separation of peptides as large as insulin on 5-μm and 10-μm bonded-phase packings indicates that the resulting h v plots for these compounds are within a factor of 2 in h, relative to similar plots for the columns in Table I. This too suggests that with proper attention to suppressing secondary retention, column efficiency for these samples will not be seriously lower than for small model compounds, such as the phthalates used here.

CONCLUSIONS

The present investigation has shown that the Knox equation (eqn. 1) provides an adequate description of column efficiency for different separation conditions and different column configurations. However, the common assumption that the coefficients A–C of this equation can be taken as roughly constant over a wide range of conditions is not true. For bonded-phase columns, we observed that B increases markedly as solute k' values are increased, and C shows a corresponding decrease with increasing k'. These effects are due mainly to diffusion of solute molecules along the bonded-phase surface, which in turn increases mass transfer within the pores of the particle. Similar trends of B and C with k' were observed for silica columns, but the effects are less pronounced, due to ten-fold slower diffusion of solute molecules along the silica surface. Values of C (for the same value of k') can vary by as much as 20-fold as a result of differences in surface diffusion coefficients. These differences in values of B and C as a function of column type and solute k' values can be quantitatively correlated in terms of an expanded form of the usual equations for B and C as a function of separation conditions. Thus, a detailed and quantitative model is now available for interpreting and predicting experimental values of B and C.

A number of practical conclusions can also be drawn from the present work. First, it was possible to pack a wide range of particle types into columns that gave minimum h values in the range of 1.6–2.2 particle diameters; *i.e.*, having A values in the range of 0.5–0.6 for bonded-phase columns and 0.7–0.8 for silica columns. These Zorbax particles were spherical in form with quite a narrow particle-size range; other particles may not perform as well. Second, it was found that the combination of particle pores smaller than 10 nm with alkyl-phases longer than C_8 gave three- to five-fold larger C values and correspondingly poorer column efficiency. This effect appears due to restricted diffusion of solute molecules in pores that are "clogged"

with the alkyl-bonded phase. Finally, the present work forms a basis for the rational design of a minimum set of optimum column configurations for practical applications.

APPENDIX I

Rejection of "bad" data points and effects on values of A

Anomalous data points were observed in some plots of h *vs.* v for large values of v. These data points were characterized by one or more of the following features:

(1) Values of h that deviated by large, positive amounts from the best fit of eqn. 1 to all of the data for a given h–v plot.

(2) Large variability in replicate determinations of a second-moment h value (first-moment values were generally much more precise).

(3) Second-moment values of h that were 20% or more greater than first-moment values, with consequent tailing of the original band.

(4) Corrections to h for the system time constant that exceeded 0.4 particle diameters (very narrow bands).

When conditions 2, 3 and/or 4 held for a particular value of h, that data point was discarded before fitting the data to eqn. 1. Discarded data usually involved points obtained with small-particle (3-μm) columns and/or small k' values ($k' < 3$), as well as rather large v values ($v > 30$). It is believed that these artifactual second-moment h values arise in part as a result of the inability of the data system to cope with very narrow bands ($4\sigma < 2$ sec), but other effects cannot be ruled out. Anomalous data points found by us are illustrated in Figs. 2a and b, where the dark circles and squares were rejected on the basis of the above criteria.

When d_p is small (*e.g.*, 3 μm) and/or k' is small ($k' < 5$), rejection of data points results for rather small values of v in most cases studied by us. This is seen in Fig. 2b for the 3-μm Zorbax-SIL column, where the maximum value of v for good data is about 6. As a result of this restriction in the range of v values, values of A become less accurately measurable. In fact, for this case, we have observed a systematic decrease in A for smaller d_p and/or k'. These trends are illustrated in Table AI.

For the Zorbax-C_8 column of Table AI, it is observed that values of A for the two particle sizes agree well for $k' = 11.5$ and/or $d_p = 5.67$ ($A = 0.51 \pm 0.08$). However, the value of A for $d_p = 3.04$ μm and $k' = 2.2$ is much smaller (0.25). The same pattern is observed for the Zorbax-SIL columns, where A is 0.73 ± 0.06 for the large k' and/or large d_p systems, but only 0.32 for $d_p = 3.04$ μm and $k' = 2.2$. Finally, for the 3.04-μm Zorbax-C_{18} column, values of A are actually negative for $k' = 1.04$, but approach a constant value of about 0.5 for k' greater than 5.

We believe that the lower values of A observed for small d_p and/or k' values are artifactual in nature, and are related to limitations in data processing which generate "bad" h values as in Fig. 2 (and discussed above). Accordingly, for this range of d_p and/or k' values, we have chosen to determine the value of A prior to applying eqn. 1 to a given h v data-set (for the purpose of measuring B and C for that data set). The value of A chosen is taken from the same column type (only d_p varying) for larger values of k' and/or d_p. Thus, in Table AI, a value of A equal to about 0.5 would be taken for the C_8 and C_{18} columns (actual value 0.55), and about 0.7 for the silica column (actual value 0.76). In Table I, the fit of eqn. 1 to experi-

TABLE AI

ARTIFACTUAL DECREASE IN VALUES OF A FOR SMALLER d_p AND/OR k' VALUES

Column	d_p	A	
		k' = 2.2	k' = 11.5
Zorbax C_8 (narrow-pore)	3.04	0.25	0.50
	5.67	0.44	0.59
Zorbax-SIL	3.04	0.32	0.79
	5.67	0.68	0.73

	k'	A
Zorbax-C_{18} (3.04 μm)	1.4	−0.31
	2.3	0.15
	3.6	0.34
	5.5	0.47
	19.9	0.49

mental h *vs* v data sets is presented both ways, when values of A were predetermined in this fashion.

APPENDIX II

Further examination of $\tilde{D}_p$ (from B term) vs. $\rho\tilde{D}_p$ (from C term)

At first glance, the conclusion from Fig. 5 and eqn. 8a appears physically unreasonable, namely that the effective diffusion coefficient for the solute inside the packing particle is different for the B term (equal to $\tilde{D}_p$) *vs* for the C term (equal to $\rho\tilde{D}_p$). After all, the same molecules are involved in each case, and their individual diffusion characteristics are the same regardless of whether the B term or C term is involved. Another argument in favor of just this conclusion is, therefore, worthwhile.

We can first assume that there are, in fact, two regions within the particle, corresponding to regions i plus ii and region iii of Fig. 5. Let the time spent by the average solute molecule in region iii be y, and the remaining time spent in regions i plus ii be $(1 - y)$; normally, y can be assumed to be small ($\ll 1$). Let the effective diffusion coefficient in regions i plus ii be $\tilde{D}'_p$, and let it be $\tilde{D}'_{pr}$ in the restricted region iii; $\tilde{D}'_{pr} \ll \tilde{D}_p$. We will assume that the k' value for the solute in regions i plus ii *vs.* region iii is the same, but this is not essential to the following argument. The actual migration of a solute molecule through the column will involve successive (small) times spent in either region i plus ii or in region iii. During each of these times, the solute band will broaden further as a result of terms A, B and C, as they apply in that region (eqn. 1). Now, it does not matter in what order the solute molecule(s) spend time in each region during migration of the molecule through the column. Therefore, the actual situation involving successive interchange of the solute molecule between different regions is equivalent to migration of the molecule first through regions i plus ii, followed by migration through region iii. This is equivalent to dividing up the column into lengths, y (region iii) and $1 - y$ (regions i plus ii). The

average value of H, applicable to the whole column can then be calculated as a function of H values for regions i plus ii and for region iii[2,38]:

$$\bar{H} = H_1(y) + H_2(1 - y), \tag{A1}$$

or

$$\bar{h} = h_1 y + h_2(1 - y). \tag{A2}$$

Here, $\bar{h}$ is the overall (average) value of h for the column, h_1 is the value that applies to region iii, and h_2 is the value that applies to regions i plus ii. We assume that $y \ll 1$.

For the B term, from eqn. 6a and eqn. A2, we can obtain

$$h = 2\gamma x/v + (2\gamma[1 - x]/vD_m)(yD'_{pr} + [1 - y]D'_p) \tag{A3}$$

Since both y and D'_{pr} are small compared to $(1 - y)$ and D'_p, eqn. A3 becomes equivalent to eqn. 6b with $D'_p \approx D_p$. That is, the effect of restricted diffusion in region iii has a minimal effect on the value of B.

The situation for the C term is altogether different. Thus, similar arguments as above lead to the expression

$$C = [1/30\gamma(1 - x)]\,[(1 + k' - x)/(1 + k')]^2\, D_m[(y/D'_{pr}) + (1 - y)/D'_p]$$

$$= C_1\,[(y/D'_{pr}) + (1 - y)/D'_p] \tag{A4}$$

With $D'_{pr} \ll D'_p$, it is seen that C from eqn. A4 no longer yields approximately the same value of C as does eqn. 8. In general, the resulting value of C will be substantially larger as a result of restricted diffusion in region iii, which is equivalent to a value of ρ in eqn. 8a that is less than 1.

A simple numerical example may show the above conclusion more clearly. Let the value of y equal 0.05, and let $D'_{pr} = 0.01\ D'_p$. Then the resulting ratios of B and C values *vs.* the case of unrestricted diffusion can be seen equal to:

$$B/B\ (\text{unrestricted}) = 0.95 + 0.0005 = 0.9505$$

(*i.e.*, about the same value of B in both cases). And

$$C/C\ (\text{unrestricted}) = (0.05/0.01) + 0.95 = 5.95.$$

Thus, the present model clearly shows that restricted diffusion in region iii will have little effect on B (as long as y is small), but can have a major effect on C. The latter example then yields a value of ρ equal to $0.9505/5.95 = 0.16$.

APPENDIX III

Derivation of experimental values of ρ in Tables I and IV and calculation of C values in Fig. 4

An example will be given of each of these calculations. Consider the case of

the 6-nm-pore Zorbax C_{18} column in Table I (d_p = 3.04 μm). The value of x for this column is 0.8 (Table IV; other values of x are 0.70 for Perkin-Elmer C_{18}, 0.71 for Supelco C_8 and 0.73 for Supelco C_{18}). The values of a and b in eqn. 7a are 1.1 and 0.39, respectively (see Fig. 3a); corresponding values for other columns are silica, 0.9 and 0.03; C_8 17-nm, 1.1 and 0.49. Remaining bonded-phase columns of Table I are assumed to be intermediate between the latter two bonded-phase columns, having a equal 1.1 and b equal 0.44.

With the above data for the 6-nm-pore C_{18} Zorbax column, we can calculate ρ, given experimental values of k' and C for some solute–mobile phase combination. Take the case (Table I) of k' equal 5.5 and C equal 0.12. We first calculate B from eqn. 7a: 1.1 + 5.5 × 0.39 = 3.25. We next calculate $\tilde{D}_p/D_m$ from eqn. 7: (3.25/1.28) − 0.8/(1 − 0.8) = 8.70. Inserting these various values into eqn. 8a then yields

$$\begin{aligned}\rho &= [1/30\gamma(1 - x)]\,[(1 + k' - x)/(1 + k')]^2\,(D_m/\tilde{D}_p)/C \\ &= [1/(30 \times 0.64 \times 0.2)]\,[(1 + 5.5 - 0.8)/(1 + 5.5)]^2/8.70 \times 0.12 \\ &= 0.192\end{aligned}$$

The calculation of C proceeds similarly. For the same example, we have an average ρ value of 0.21 (Table V). We proceed as above to calculate B = 3.25 and $\tilde{D}_p/D_m$ = 8.70 for k' = 5.5. Inserting these values into eqn. 8a gives

$$\begin{aligned}C &= [1/(30 \times 0.64 \times 0.2)]\,[(1 + 5.5 - 0.2)/(1 + 5.5)]^2/8.7 \times 0.21 \\ &= 0.110.\end{aligned}$$

SYMBOLS

a, b	Constants in eqn. 7a (see Fig. 3); values for columns of Table I given in the text
A, B, C	Knox parameters, defined in eqn. 1 (see text)
d_p	Average particle diameter (cm)
D_m	Solute diffusion coefficient (cm²/sec) in mobile phase outside the particle
D_p	Solute diffusion coefficient (cm²/sec) in mobile phase inside the particle
$\tilde{D}_p$	Effective solute diffusion coefficient inside the particle, equal to combined diffusion coefficient in mobile and stationary phases; see eqns. 6a–7
D_s	Solute diffusion coefficient (cm²/sec) within the stationary phase (surface diffusion along pore walls)
h	Reduced plate height, equal to H/d_p
H	Plate height, equal to L/N (cm)
k'	Solute capacity factor
L	Column length (cm)
N	Column plate number determined by second-moments method
u	Mobile phase velocity, equal L/t_0 (t_0 is column dead-time) (cm/sec)
x	Fraction of mobile phase in the column that is outside the particles
γ	Tortuosity factor for solute diffusion in the column; value of 0.64 assumed here
γ_o	Value of γ for diffusion outside the particles
γ_p	Value of γ for diffusion in the particle pores
γ_s	Value of γ for diffusion along the pore walls

ν Mobile phase reduced velocity, equal $u\, d_p/D_m$

ρ Restricted diffusion factor, which, when multiplied by $\tilde{D}_p$ yields the actual diffusivity of solute molecules, as they affect the C term of eqn. 1; $\rho\tilde{D}_p$ is the apparent diffusion coefficient for solute molecules moving into and out of the stationary phase (see discussion of eqn. 8a)

σ Square root of the variance contributed by extra-column volumes to total peak variance (referred to as σ_{ec}) in ref. 10)

τ Time constant of the HPLC system[10]; the total non-column contribution to band variance is $\sigma^2 + \gamma^2$

REFERENCES

1 L. R. Snyder and J. J. Kirkland, *Introduction to Modern Liquid Chromatography*, Wiley-Interscience, New York, 1979, 2nd ed., Chs. 2 and 5.
2 J. C. Giddings, *Dynamics of Chromatography*, Marcel Dekker, New York, 1965.
3 J. H. Knox and M. Saleem, *J. Chromatogr. Sci.*, 7 (1969) 614.
4 G. J. Kennedy and J. H. Knox, *J. Chromatogr. Sci.*, 10 (1972) 549.
5 J. H. Knox and A. Pryde, *J. Chromatogr.*, 112 (1975) 171.
6 J. H. Knox, *J. Chromatogr. Sci.*, 15 (1977) 352.
7 G. Guiochon, in Cs. Horváth (Editor) *High-performance Liquid Chromatography*, Vol. 2, Academic Press, New York, p. 1.
8 L. R. Snyder, *J. Chromatogr. Sci.*, 15 (1977) 441.
9 J. R. Gant, J. W. Dolan and L. R. Snyder, *J. Chromatogr.*, 185 (1979) 153.
10 R. W. Stout, J. J. DeStefano and L. R. Snyder, *J. Chromatogr.*, 261 (1983) 189.
11 J. J. Kirkland, *J. Chromatogr.*, 83 (1973) 149; *J. Chromatogr. Sci.*, 10 (1972) 593.
12 I. Halász, H. Schmidt and P. Vogtel, *J. Chromator.*, 126 (1976) 19.
13 J. H. Done and J. H. Knox, *J. Chromatogr. Sci.*, 10 (1972) 606.
14 Cs. Horváth and H. J. Lin, *J. Chromatogr.*, 149 (1978) 43.
15 I. Halász, R. Endele and J. Asshauer, *J. Chromatogr.*, 112 (1975) 37.
16 K. K. Unger, W. J. Messer and K. F. Krebs, *J. Chromatogr.*, 149 (1978) 1.
17 J. H. Knox, G. R. Laird and P. A. Raven, *J. Chromatogr.*, 122 (1976) 129.
18 J. C. Chen and S. G. Weber, *Anal. Chem.*, 55 (1983) 127.
19 J. H. Knox and H. P. Scott, *J. Chromatogr.*, 282 (1983) 279.
20 J. H. Knox and L. McLaren, *Anal. Chem.*, 36 (1964) 1477.
21 L. R. Snyder and H. Poppe, *J. Chromatogr.*, 184 (1980) 363.
22 L. R. Snyder, *J. Chromatogr.*, 255 (1983) 3.
23 L. R. Snyder, in Cs. Horváth (Editor) *High-performance Liquid Chromatography*, Vol. 3, Academic Press, New York, 1983.
24 W. W. Yau, J. J. Kirkland and D. D. Bly, *Modern Size-exclusion Liquid Chromatography*, Wiley-Interscience, New York, 1979, p. 89.
25 R. R. Walters, *J. Chromatogr.*, 249 (1982) 19.
26 J. H. Knox and F. McLennan, *J. Chromatogr.*, 185 (1979) 289.
27 M. E. van Kreveld and N. van den Hoed, *J. Chromatogr.*, 149 (1978) 71.
28 R. Groh and I. Halász, *Anal. Chem.*, 53 (1981) 1325.
29 K. Karch, I. Sebestian and I. Halász, *J. Chromatogr.*, 122 (1976) 3.
30 W. Engelhardt, B. Dreyer and H. Schmidt, *Chromatographia*, 16 (1982) 11.
30a H. Engelhardt and N. Weigand, *Anal. Chem.*, 45 (1973) 1149.
31 Cs. Horváth, in E. Heftmann (Editor), *Chromatography*, Elsevier, Amsterdam, Oxford, New York, 1983, Ch. 3.
32 L. R. Snyder, *J. Chromatogr. Sci.*, 7 (1969) 352.
33 J. L. DiCesare, M. W. Dong and L. S. Ettre, *Introduction to High-Speed Liquid Chromatography*, Perkin-Elmer, Norwalk, CT, 1982.
34 W. Kutner, J. Debowski and W. Kemula, *J. Chromatogr.*, 218 (1981) 45.
35 R. Eksteen, private communication.
36 J. H. Knox and G. R. Laird, *J. Chromatogr.*, 122 (1976) 17.
37 J. L. Meek and Z. L. Rossetti, *J. Chromatogr.*, 211 (1981) 15.
38 J. Kwok, L. R. Snyder and J. C. Sternberg, *Anal. Chem.*, 40 (1968) 118.